CrossMark

Uncertainty budget for determinations of mean isomer shift from Mössbauer spectra

Jeppe Fock[1,4] · **Lara Katrina Bogart**[2] · **Oliver Posth**[3] ·
Mikkel Fougt Hansen[1] · **Quentin A. Pankhurst**[2] ·
Cathrine Frandsen[4]

Abstract The magnetite/maghemite content within iron oxide nanoparticles can be determined using the mean isomer shift ($\bar{\delta}$). However, accurate characterisation of the composition is limited by the uncertainty associated with $\bar{\delta}$. We have identified four independent sources of uncertainty and developed a quantitative expression for the uncertainty budget. Sources of uncertainty are categorised as follows: that from the fitting of the Mössbauer spectrum (σ_{fit}), that of the calibration of the α-Fe reference spectrum (σ_{cal}), thermal corrections to the spectrum due to second order Doppler shift (SODS) ($\sigma_{\Delta\delta}$) and other experimental errors (σ_{err}). Each contribution is discussed in detail using ^{57}Fe Mössbauer spectra obtained from an iron oxide nanoparticle system at temperatures between 16 K and 295 K on different spectrometers in two different laboratories.

This article is part of the Topical Collection on *Proceedings of the International Conference on the Applications of the Mössbauer Effect (ICAME 2015), Hamburg, Germany, 13–18 September 2015*

✉ Jeppe Fock
jepf@nanotech.dtu.dk

Cathrine Frandsen
fraca@fysik.dtu.dk

1   Department of Micro- and Nanotechnology, DTU Nanotech, Building 345 East, Technical University of Denmark, DK-2800 Kongens Lyngby, Denmark

2   UCL Healthcare Biomagnetics Laboratory, University College London, 21 Albemarle Street, London, W1S 4BS, UK

3   Department 8.2 Biosignals, Physikalisch-Technische Bundesanstalt, Abbestr. 2-12, 10587 Berlin, Germany

4   Department of Physics, DTU Physics, Building 307, Technical University of Denmark, DK-2800 Kongens Lyngby, Denmark

🖄 Springer

1 Introduction

[57]Fe Mössbauer spectroscopy is one of the few methods able to distinguish between magnetite (Fe_3O_4) and maghemite (γ-Fe_2O_3), where both the chemical shift and the presence or absence of characteristic lines identify the respective type of iron oxide. However, sometimes the spectral parts of the two phases are not easily distinguishable, e.g., in case of non-stoichiometric magnetite or superparamagnetic relaxation. It has been proposed that the magnetite/maghemite content can be determined by the analysis of the mean isomer shift [1–3].

The accuracy of the magnetite/maghemite content determination depends on the uncertainty of the determined mean isomer shift. All of the above mentioned works assume a constant uncertainty, of 0.005, 0.01 and 0.01 mm/s, respectively. However, the uncertainty on the determination on the isomer shift depends strongly on the complexity of the Mössbauer spectrum, the sharpness of the lines in the spectrum, and a number of other parameters that have to be taken into account. Therefore, the assumption of a constant uncertainty is inadequate and may lead to erroneous conclusions.

Different methods for determining the mean isomer shift exist, but not all are suitable. Calculating the mean isomer shift $\overline{\delta}$ as the numerical calculated mean of the Mössbauer absorption spectrum (the first moment) is not a feasible route, because the first moment of a Lorentzian is not well defined [4]. In addition, a slight slope in the background of the spectrum will introduce large errors in a numerical calculation. Instead, the mean isomer shift can be found by fitting the spectra with sextets and doublets and subsequently calculating the area weighted mean of the isomer shifts from all N components [1]:

$$\overline{\delta} = \frac{\sum_i^N A_i \delta_i}{A} \qquad (1)$$

δ_i is the isomer shift of the i-th component with area A_i, and $A = \sum_i^N A_i$ is the total area.

In the following we will develop the uncertainty budget for the mean isomer shift determination and illustrate the different contributions to the uncertainty with examples.

2 Experimental details

[57]Fe Mössbauer spectroscopy was carried out at both the Technical University of Denmark (DTU) and University College London (UCL).

[57]Fe Mössbauer spectroscopy at DTU was performed using conventional constant acceleration spectrometers with sources of [57]Co in rhodium. Calibration was carried out using a 12.5 μm foil of α-Fe at room temperature (RT). Spectra obtained at temperatures down to 16 K were recorded in a close cycle helium refrigerator from APD Cryogenics. The nanoparticle system was measured as a frozen dispersion ($T \leq 250$ K).

[57]Fe Mössbauer spectroscopy at UCL was performed at RT using a SeeCo W302 spectrometer. Spectra were recorded using a [57]Co in rhodium matrix driven at constant acceleration using a triangluar waveform, and recorded in a SeeCo W202 multi-channel analyser (1024 channels). All spectra were folded relative to an α-Fe foil also at RT. An example of the calibration measured at UCL is shown in Fig. 3. The nanoparticle system was air dried over the course of a week and mixed with sucrose in a pestle and mortar to form a paste.

The nanoparticle used in this work was the SP02 nanoparticle system described previously in [5]. The sample consists of polystyrene spheres decorated with iron oxide

nanocrystals with a nominal size 8 nm. DC-magnetometry measurements at 300 K show this system to be in the superparamagnetic state [5].

3 Uncertainty budget

The uncertainty associated with the mean isomer shift, $\sigma_{\bar{\delta}}$, can be divided up into four contributions:

1. fitting of the Mössbauer spectrum, σ_{fit}
2. calibration of the α-Fe reference spectrum, σ_{cal}
3. post treatment of the data (e.g., taking account of second order Doppler shift, SODS), $\sigma_{\Delta\delta}$
4. experimental errors such as large derivations from a flat background or non-linear velocity-channel calibration; σ_{err}

These four contributions are uncorrelated and consequently, they can be treated independently:

$$\sigma_{\bar{\delta}}^2 = \sigma_{\text{fit}}^2 + \sigma_{\text{cal}}^2 + \sigma_{\Delta\delta}^2 + \sigma_{\text{err}}^2. \tag{2}$$

Each contribution is described here in detail. Section 3.1 describes the procedure to obtain the uncertainties and correlations of the fitted parameters (e.g., the areas and isomer shifts of the spectral components). In addition, it describes how these uncertainties propagate into the uncertainty in the isomer shift σ_{fit}. Section 3.2 describes how the uncertainties in the calibration parameters are obtained, and how they propagate to σ_{cal}. Section 3.3 describes how to correct for second order Doppler shift (SODS), and how the associated uncertainty propagates into $\sigma_{\Delta\delta}$. Finally, other experimental errors σ_{err} are qualitatively discussed in Section 4.

3.1 Fitting of Mössbauer spectra

To find the mean isomer shift of a sample it is not necessary to fit with the correct physical model. However, it is important that the samples are thin and texture-free and that areas of the lines in the sextets are kept in ratios $3:2:1$. If the area ratios are $3:x:y$, the mean isomer shift of the components in the sextets will have a component proportional to $E_q(3-x-y)$, where E_q is the quadrupole interaction. Thus, a nonzero quadrupole interaction is only allowed if $x+y=3$. This can be satisfied by enforcing an area ratio of $3:2:1$ for the three pairs of lines in a sextet. Qualitatively, this can be explained by the fact that the quadrupole interaction shifts the innermost four lines in the opposite direction of the two outermost lines (see Fig. 1), and therefore the area of the innermost four lines should be equal to that of the two outermost lines to preserve the mean isomer shift.

To calculate the mean isomer shift, the areas and isomer shifts of the N spectral components are required as shown in (1). The parameters $(\vec{p} = A_1, \ldots, A_N, \delta_1, \ldots, \delta_N)$ describe, among others, the model $f(v_i, \vec{p})$ which is fitted to the data. It is not necessary that $f(v_i, \vec{p})$ describes the different Fe sites in the crystal correctly. However, $f(v_i, \vec{p})$ should produce a good fit to the data.

The optimal values of the parameters $\vec{p}^*$ are obtained by minimization of $\chi^2 = \sum_i (f_i(\vec{p}))^2$, where the fitting function $f_i(\vec{p})$ is

$$f_i(\vec{p}) = w_i (s_i - f(v_i, \vec{p})). \tag{3}$$

Here, i is the channel number, s_i is the count in the i-th channel of the folded spectrum, and w_i is the weighting of the i-th data point. If the spectrum is folded around an integer or

Fig. 1 Schematic of the movement of the peaks in a sextets when the quadrupole interaction increases from 0 mm/s (*solid line*) to 0.8 mm/s (*dotted line*). The arrows indicates the direction of the shift of the peaks
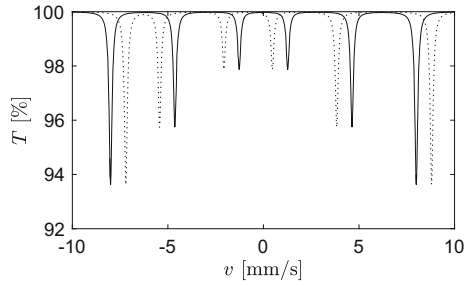
half integer channel number the count numbers in the folded spectrum (s_i) are uncorrelated. w_i can in this case be calculated as $w_i = 1/\sigma_{s_i}$ where σ_{s_i} is the standard deviation. For the nuclear events of emission and absorption of gamma rays, the uncertainty of the count number is governed by Poisson statistics - thus the standard deviation is simply $\sigma_{s_i} = \sqrt{s_i}$. If the spectrum is not folded over an integer or half integer channel number, the value of s_i become correlated. For the correlated case the weighting is described by a matrix multiplication and (3) becomes $f_i(\vec{p}) = \sum_j W_{ij}(s_j - f(v_j, \vec{p}))$[6]. **W** can be calculated as the Cholesky decomposition of the inverse folded channel covariance matrix: $\mathbf{W}^T\mathbf{W} = \mathbf{C}^{-1}$ (see SI).

When the fitting function is correctly scaled as described above, the covariance matrix for the fitted parameters is found by $\Sigma_{\vec{p}} = \left(\mathbf{J}(\vec{p}^*)^T\,\mathbf{J}(\vec{p}^*)\right)^{-1}$ [7]. The Jacobian matrix **J** is:

$$\mathbf{J}(\vec{p}) = \begin{bmatrix} \frac{\partial f_1(\vec{p})}{\partial A_1} & \cdots & \frac{\partial f_1(\vec{p})}{\partial \delta_N} \\ \vdots & \ddots & \vdots \\ \frac{\partial f_n(\vec{p})}{\partial A_1} & \cdots & \frac{\partial f_n(\vec{p})}{\partial \delta_N} \end{bmatrix} \qquad (4)$$

To calculate the propagation of the uncertainties to $\overline{\delta}$, we construct the Jacobian of (1) as:

$$\begin{aligned} \mathbf{J}_{\overline{\delta}} &= \begin{bmatrix} \frac{\partial \overline{\delta}}{\partial A_1} & \cdots & \frac{\partial \overline{\delta}}{\partial A_N} & \frac{\partial \overline{\delta}}{\partial \delta_1} & \cdots & \frac{\partial \overline{\delta}}{\partial \delta_N} \end{bmatrix} \\ &= \begin{bmatrix} \frac{\delta_i - \overline{\delta}}{A} & \cdots & \frac{\delta_N - \overline{\delta}}{A} & \frac{A_1}{A} & \cdots & \frac{A_N}{A} \end{bmatrix} \end{aligned} \qquad (5)$$

The uncertainty of the mean isomer shift is then calculated by first-order error propagation [8] as:

$$\sigma_{\text{fit}}^2 = \mathbf{J}_{\overline{\delta}}\Sigma_{\vec{p}}\mathbf{J}_{\overline{\delta}}^T. \qquad (6)$$

3.1.1 Fitting of Mössbauer spectra - example

Figure 2a shows a Mössbauer spectrum obtained at 16 K with an asymmetric sextet with narrow lines. The spectrum has been fitted using four sextets with Voigt line-shapes. The widths of the Gaussians lines were scaled to represent a distribution of magnetic hyperfine fields [9], where the hyperfine field distributions are approximated with up to two Gaussian components. Fitting parameters are provided in Table S1. Although the uncertainty of the individual components are all larger than 0.006 mm/s, the uncertainty on the mean isomer shift is only 0.002 mm/s. This is due to *correlations* between the fitting parameters.
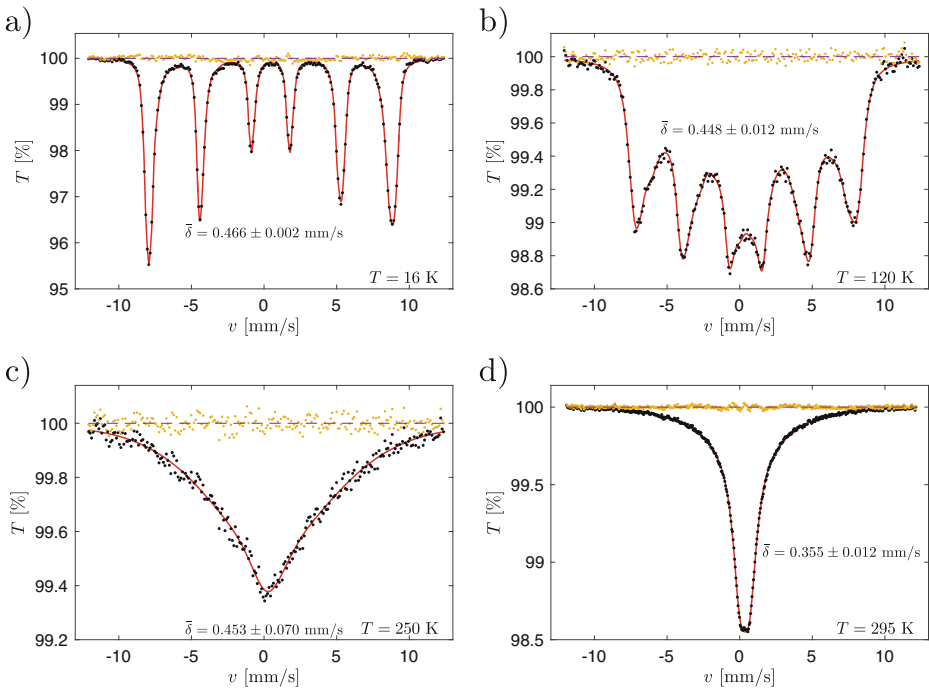
a)

b)

c)

d)

Fig. 2 Mössbauer spectra of a SP02 nanoparticle dispersion measured at (**a**) $T = 16$ K, (**b**) $T = 120$ K, (**c**) $T = 250$ K. (**d**) Mössbauer spectrum of a sample of dried SP02 particles measured at $T = 295$ K. The (**a**)-(**c**) spectra have similar count numbers $\left(\simeq 1 \cdot 10^7\right)$, and (**d**) has a count number of $\simeq 7 \cdot 10^7$

For example, if the spectral area of one sub-component increases, then the area of another sub-component must decrease to keep the total area constant. The uncertainty without correlations is 0.006 mm/s, deduced by setting off-diagonal elements in the covariance matrices to zero.

For the broader spectrum obtained at 120 K (Fig. 2b), the uncertainties on the mean isomer shift obtained with and without correlation are 0.012 mm/s and 0.022 mm/s, respectively. The positions of the individual lines have high uncertainties (Table S2), which result in a high uncertainty if correlations are not included. When correlations between the fitting parameters are included, the uncertainty decreases by a factor of 2.

In some cases (e.g., for some temperatures), the obtained spectrum has very broad lines (Fig. 2c). Consequently, the determination of $\bar{\delta}$ has a much higher uncertainty. The large correlation between the spectrum and the baseline, which is reflected in a normalized correlation coefficient close to 0.5 (Table S3), can partly be responsible for the large uncertainty of the mean isomer shift. This could potentially be improved by choosing a broader velocity range or by choosing a measurement temperature where the spectrum has narrow lines. For this case, as $\bar{\delta}$ depends only weakly on the magnetite/maghemite content [2], the uncertainty on the magnetite/maghemite ratio is also very high. In practise, the uncertainty on this ratio becomes so large that the spectrum at this temperature does not provide any useful information.

Table 1 (Table S5) summarise the obtained uncertainties for all four spectra including (excluding) correlations.

Table 1 The contributions to the uncertainty from the fitting σ_{fit}, calibration σ_{cal} and the SODS correction $\sigma_{\Delta\delta}$ to 295 K, as well as the total uncertainty of the mean isomer determination $\sigma_{\bar{\delta}}$ for spectra of SP02 nanoparticles obtained at 16 K (Fig. 2a), 120 K (Fig. 2b), 250 K (Fig. 2c) and 295 K (Fig. 2d). The magnetite fraction, w, was calculated as in [2]

T [K]	σ_{fit} [mm/s]	σ_{cal} [mm/s]	$\sigma_{\Delta\delta}$ [mm/s]	$\sigma_{\bar{\delta}}$ [mm/s]	w [%]
16	0.0017	0.0015	0.0059	0.0063	4 ± 1
120	0.0122	0.0015	0.0046	0.0131	5 ± 6
250	0.0704	0.0015	0.0016	0.0704	41 ± 33
295	0.0122	0.0016	0.0000	0.0123	9 ± 6

3.2 Calibration of the α-Fe reference spectrum

In addition to the uncertainty in the determination of the isomer shift from the fitting of the spectra described above, the translation from channel number to energy through the calibration adds an additional source of uncertainty. The energy/velocity of the i-th channel of the data is $v_i = (i - c_0) \cdot k$, where c_0 and k are the zero channel and calibration constant obtained from a reference spectrum (e.g. α-Fe foil). The calibration of the spectra introduces an uncertainty on velocity through the calibration values c_0 and k. A covariance matrix $\Sigma_{c_0,k}$ with non-zero off-diagonal elements describes the correlations and uncertainties of c_0 and k as

$$\Sigma_{\mathbf{c_0,k}} = \begin{bmatrix} \sigma_{c_0}^2 & \sigma_{c_0,k} \\ \sigma_{c_0,k} & \sigma_k^2 \end{bmatrix} \tag{7}$$

Here, $\sigma_{c_0}^2$ and σ_k^2 are the variances of the zero channel and calibration constant respectively, and $\sigma_{c_0,k}$ is their covariance.

To obtain the calibration values, Lorentzian functions are fitted to all twelve peaks in the unfolded reference spectrum. The fitted position of the twelve Lorentzians c_n can be related to the folding channel c_f, zero channel and calibration constant by:

$$c_l = \frac{E_l}{k} + c_0 \quad \text{for } 1 \leq l \leq 6 \tag{8a}$$

$$c_l = \frac{-E_{13-l}}{k} + c_0 + \frac{c_f}{2} \quad \text{for } 7 \leq l \leq 12, \tag{8b}$$

where E_l is the energy of the l-th line in the reference spectrum. The parameters c_0, k, c_f and their covariance matrix can be found from these equations using linear regression. Note that this method gives a non-integer folding channel.

As a consequence of the non-integer folding channel, folding of the spectrum requires interpolation of the data points. Splitting the folding channel into the integer part $c_{\bar{f}}$ and the fractional part a, the folded spectrum is expressed as:

$$s_i = n_i + (1-a)\, n_{c_{\bar{f}}-i} + a n_{c_{\bar{f}}+1-i} \quad \text{for } 1 \leq i \leq \frac{c_f}{2}, \tag{9}$$

where n_i is the count number of i-th channel in the unfolded spectrum.

To find the uncertainty propagated to $\bar{\delta}$ from the calibration uncertainties (1) has to be expressed using the calibration constants. Therefore, $\delta_l = (c_l - c_0) \cdot k$ is inserted in (1), where c_l is the channel number of the isomer shift of component l. This enables us to calculate the Jacobian:

$$\mathbf{J}_{\bar{\delta}} = \begin{bmatrix} \dfrac{\partial \bar{\delta}}{\partial c_0}, & \dfrac{\partial \bar{\delta}}{\partial k} \end{bmatrix} = \begin{bmatrix} -k, & \dfrac{\bar{\delta}}{k} \end{bmatrix} \tag{10}$$
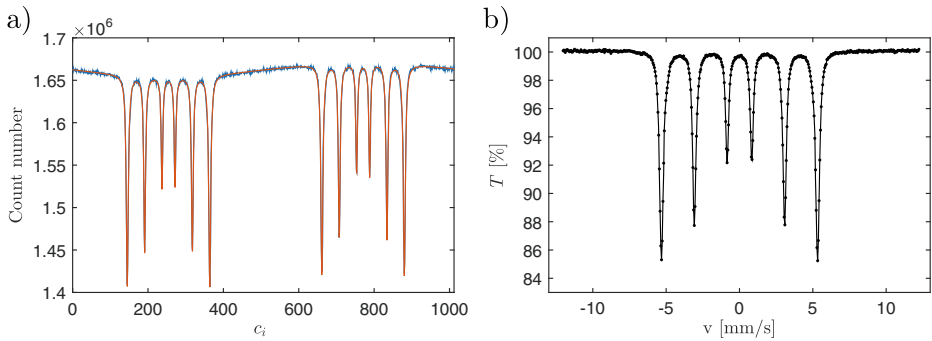
a)

b)

Fig. 3 **a** The unfolded spectrum of α-Fe foil with fitted Lorentzian functions to all peaks. **b** The folded α-Fe foil spectrum

The contribution from the calibration to the uncertainty is then calculated by first-order error propagation as

$$\sigma_{\text{cal}}^2 = \frac{\overline{\delta}^2}{k^2} \cdot \sigma_k^2 + k^2 \cdot \sigma_{c_0}^2 - 2k\overline{\delta} \, \sigma_{k,c_0}. \tag{11}$$

3.2.1 Calibration - example

Figure 3a shows the unfolded spectrum of an α-Fe foil calibration sample. Using (3.2), the calibration constants were calculated to be $k = 0.04860$ mm/s, $c_0 = 254.37$, and $c_f = 1025.14$ and the covariance matrix had the following values: $\sigma_k^2 = 2.8 \cdot 10^{-10}$ mm^2/s^2, $\sigma_{c_0}^2 = 1.3 \cdot 10^{-3}$, $\sigma_{c_0,k} = 2.7 \cdot 10^{-23}$ mm/s. Using the values of the obtained covariance matrix, the contribution to the uncertainty from the calibration was obtained as described above. Assuming zero isomer shift, as is expected for α-Fe, the uncertainty on the isomer shift was 0.0017 mm/s.

The α-Fe spectrum was folded using the obtained calibration values (Fig. 3b). Fitting the folded calibration spectrum with a sextet with the quadrupole interaction fixed to zero, we obtained an isomer shift of 0.0005 ± 0.0017 mm/s.

3.3 Second order Doppler shift correction

If the measured mean isomer shift is compared to a reference measurement performed at another temperature, a correction to the mean isomer shift is needed. In this case the temperature dependence of the reference compound must be known.

For the simplest case, the temperature dependence is only governed by the second order Doppler shift (SODS). In this case the correction can be expressed using the Debye model with a single parameter, the Debye temperature T_{D} of the compound:

$$\text{SODS(T)} = -\frac{9k_{\text{B}}T}{2mc} \left[\left(\frac{T}{T_{\text{D}}} \right)^3 \int_0^{T_{\text{D}}/T} \frac{x^3}{e^x - 1} \mathrm{d}x \right]. \tag{12}$$

Here, m is the mass of the iron nucleus, c is the speed of light and k_{B} is the Boltzmann constant.
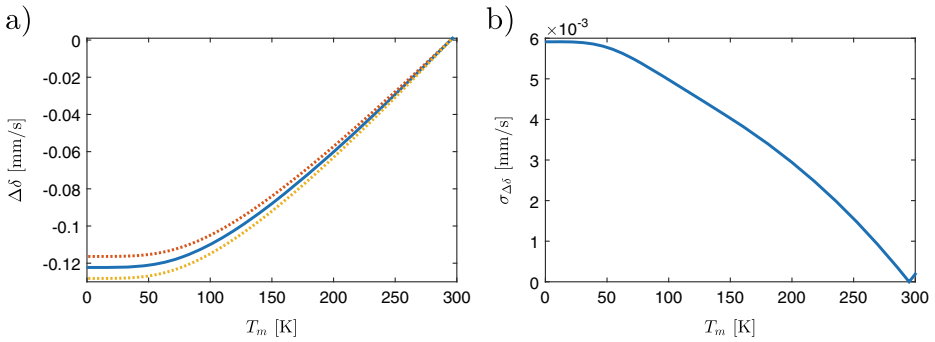
a)

b)

Fig. 4 **a** Change in the isomer shift $\Delta\delta$ due to the SODS correction of the isomer shift from T_m to 295 K. The *dotted lines* are $\Delta\delta \pm \sigma_{\Delta\delta}$. **b** Uncertainty in the SODS correction $\sigma_{\Delta\delta}$. A Debye temperature of $T_D = 416$ K $\pm$ 17 K is used in the calculation

To correct the isomer shift for the difference between the measured temperature T_m to the reference temperature T_r, we calculate the change in the isomer shift:

$$\Delta\delta = \frac{-9k_B}{2mc}\left[T_r \left(\frac{T_r}{T_D}\right)^3 \int_0^{T_D/T_r} \frac{x^3}{e^x - 1}\,dx - T_m \left(\frac{T_m}{T_D}\right)^3 \int_0^{T_D/T_m} \frac{x^3}{e^x - 1}\,dx \right] \quad (13)$$

The Debye temperature has an uncertainty, which propagates through (13) to an uncertainty in $\Delta\delta$. This propagation is given as: $\sigma_{\Delta\delta} = \left|\frac{\Delta\delta}{\partial T_D}\right| \sigma_{T_D}$. The derivative of $\Delta\delta$ with respect to the Debye temperature is calculated using the Leibniz integral rule and the product rule:

$$\frac{\partial\Delta\delta}{\partial T_D} = \frac{-9k_B}{2mc}\left[-3\left(\frac{T_r}{T_D}\right)^4 \int_0^{T_D/T_r} \frac{x^3}{e^x - 1}\,dx + 3\left(\frac{T_m}{T_D}\right)^4 \int_0^{T_D/T_m} \frac{x^3}{e^x - 1}\,dx \right. \quad (14)$$
$$\left. + \frac{1}{e^{T_D/T_r} - 1} - \frac{1}{e^{T_D/T_m} - 1} \right]$$
$$= -3\frac{\Delta\delta}{T_D} - \frac{9k_B}{2mc}\left(\frac{1}{e^{T_D/T_r} - 1} - \frac{1}{e^{T_D/T_m} - 1} \right) \quad (15)$$

3.3.1 Second order Doppler shift correction - example

The calculated mean isomer shift often has to be compared to the mean isomer shifts of some reference compounds. However, there could be differences in the experimental details between the reference compounds and the sample. If the reference compounds consist of large crystallites, spectra with narrow lines can be obtained at RT. When measuring magnetic nanoparticles showing superparamagnetic behaviour at RT, it might be necessary to cool the sample to obtain a spectrum with a low uncertainty of the mean isomer shift (cf. Section 3.1.1).

Figure 4a shows the correction needed when comparing a sample measured at T_m with reference compounds measured at RT for a SODS with a Debye temperature of $T_D = 416$ K $\pm$ 17 K (typical for magnetite, uncertainty determined from data not shown). Thus, the mean isomer value for the sample has to be corrected by up to -0.12 mm/s to

allow for comparison with a reference sample measured at 295 K. The correction introduces an additional uncertainty of up to 0.006 mm/s (Fig. 4b).

At high temperatures ($T \gtrsim 150$ K), the mean isomer correction depends approximately linearly on the temperature, $\Delta \bar{\delta} = (6.6 \cdot 10^{-4}$ mm/(sK)$) \, \Delta T$. Thus, an uncertainty on the temperature σ_T will propagate into an uncertainty on the mean isomer shift: $\sigma_{\Delta \bar{\delta}} = (6.6 \cdot 10^{-4}$ mm/sK$) \, \sigma_T$. A seasonal change in temperature of more than 5 K is not unusual in non-air conditioned laboratories. The uncertainty due to a variation in the definition of RT can result in uncertainties of more than 0.003 mm/s. Also night-to-day temperature variation can result in broadening of the spectrum and/or in an uncertainty of the mean isomer shift determination.

A comparison of the two measurements shown in Fig. 2a,b demonstrates the need to correct for the SODS. The mean isomer shift of the 120 K spectrum can be corrected to 16 K using (13): The corrected mean isomer shift is 0.453 ± 0.013 mm/s, well within the measured value of 0.466 ± 0.002 mm/s obtained from the spectrum in Fig. 2a. In this case the uncertainty of the SODS correction is small compared to the other contributions and only slightly increases the total uncertainty. However, correcting the 16 K spectrum (Fig. 2a) to 295 K, the uncertainty triples to a significant value of 0.006 mm/s.

4 Discussion and conclusion

We have shown how the uncertainties from the fitting, the calibration and the temperature calibration propagate to the total uncertainty of the mean isomer shift. The uncertainty originating from experimental errors σ_{err} is difficult to quantify in a generic way and such approaches may result in erroneous conclusions. Thus, it is important when comparing the mean isomer shifts to ensure that the Mössbauer spectrum has a flat non-sloping background in addition to obtaining sufficient counting statistics (see an example in supplementary information).

Contamination of the sample with other iron containing compounds may introduce a systematic change of $\bar{\delta}$, and if pure magnetite and maghemite phases are assumed, a contamination will introduce a systematic error on the ratio between these two phases determined from the mean isomer shift.

Table 1 compares the different contributions to the uncertainty on the mean isomer determination for three spectra of a SP02 nanoparticle dispersion obtained at 16 K, 120 K and 250 K and one spectrum of a SP02 nanoparticle powder obtained at 295 K. The SODS have been corrected to 295 K for all spectra. It is seen that for the spectrum obtained at 16 K, the SODS correction dominates, whereas for the higher temperatures the uncertainty in the fitting of the spectrum is largest. Thus, a minimum in the mean isomer uncertainty must exist at a temperature between 16 K and 120 K.

For all cases, the uncertainty introduced by the calibration is small and has only a minor impact on the total uncertainty of $\bar{\delta}$.

The total absorption decreases with increasing temperature due to the temperature dependence on the recoil-free fraction of absorbed gamma rays. Together with the broadening of the lines for the nanoparticle dispersion (Fig. 2a-c) this results in an increasing mean isomer shift uncertainty. The decrease in the total absorption for the 295 K sample, due to the recoil-free fraction, is compensated by the fact that the spectrum is almost completely collapsed into a doublet (Table S4). This, and possibly also a higher Fe concentration in the powder sample, results in a larger maximal absorption. The low uncertainty observed for

the 295 K sample can be explained by the larger absorption as well as the narrow line of the doublet.

Table 1 also shows the magnetite content calculated using the expression provided in [2], which also includes the uncertainty as deduced from the mean isomer shift. The uncertainty in the mean isomer shift for the broad-line 250 K spectrum results in a magnetite content uncertainty of $\pm$ 33 %. Therefore, in practice the magnetite/maghemite content is close to being undetermined based on this spectrum. The lower uncertainties in the mean isomer spectra obtained at 16 K, 120 K and 295 K make these spectra suitable for magnetite/maghemite determination. The magnetite fraction values determined from these spectra agree within their respective uncertainties.

This agreement indicates, since the samples were measured in two different laboratories and using different sample preparation (freeze dried powder and frozen dispersion), that sources of experimental error are insignificant. For example, we do not observe oxidation upon air drying of the liquid sample. Finally, we note that the definition of room temperature is relevant. A variation of 5 K in the definition of RT causes a variation of the mean isomer shift corresponding to a 1.5 % variation in the magnetite content.

In contrast to other studies using a constant uncertainty for the isomer shift, we have explored the different origins for the uncertainty. Furthermore, we have summarised the mathematical background in order to assess the different contributions quantitatively. The mathematical models have been applied to Mössbauer studies performed on magnetite/maghemite nanoparticles with the aim to derive the total uncertainty of the isomer shift in these systems.

References

1. Santoyo Salazar, J., Perez, L., de Abril, O., Truong Phuoc, L., Ihiawakrim, D., Vazquez, M., Greneche, J.-M., Begin-Colin, S., Pourroy, G.: Magnetic iron oxide nanoparticles in 10-40 nm range: Composition in terms of magnetite/maghemite ratio and effect on the magnetic properties. Chem. Mater. **23**, 1379–1386 (2011)
2. da Costa, G.M., Blanco-Andujar, C., De Grave, E., Pankhurst, Q.A.: Magnetic nanoparticles for in vivo use: a critical assessment of their composition. J. Phys. Chem. B **118**, 11738–46 (2014)
3. Almeida, T.P., Muxworthy, A.R., Kasama, T., Williams, W., Damsgaard, C., Frandsen, C., Pennycook, T.J., Dunin-Borkowski, R.E.: Effect of maghemization on the magnetic properties of nonstoichiometric pseudosingle-domain magnetite particles, Geochemistry, Geophys. Geosystems, pp. n/a–n/a **16**, 2969–2979 (2015)
4. Ohakwe, J., Osu, B.: The existence of the moments of the Cauchy distribution under a simple transformation of dividing with a constant. Theor. Math. Appl. **1**(1), 27–35 (2011)
5. Bogren, S., Fornara, A., Ludwig, F., del Puerto Morales, M., Steinhoff, U., Hansen, M., Kazakova, O., Johansson, C.: Classification of magnetic nanoparticle systems-synthesis, standardization and analysis methods in the nanomag project. Int. J. Mol. Sci. **16**(9), 20308–20325 (2015)
6. Tellinghuisen, J.: On the least-squares fitting of correlated data: removing the correlation. J. Mol. Spectrosc **165**, 255–264 (1994)
7. van de Geer, S.A.: Least squares estimation. In: Encycl. Stat. Behav. Sci., pp. 1041–1045, Chichester, UK: John Wiley & Sons Ltd (2005)

8. Joint Committee for Guides in Metrology: Evaluation of measurement data – supplement 2 to the guide to the expression of uncertainty in measurement – extension to any number of output quantities. JCGM **102**, 2011 (2011)
9. Lagarec, K., Rancourt, D.: Extended Voigt-based analytic lineshape method for determining n-dimensional correlated hyperfine parameter distributions in mössbauer spectroscopy. Nucl. Instruments Methods Phys. Res. Sect. B Beam Interact. with Mater. Atoms **129**(2), 266–280 (1997)